PROGRAM RADA

Utorak 18.10.2005.	
09:00÷11:00	Registracija učesnika
11:00÷11:30	Otvaranje i pozdravna reč
11:30÷13:30	**Predavanja po pozivu** ***PREDSTAVLJANJE GENERALNOG POKROVITELJA***
13:30÷14:00	Koktel
14:00÷16:00	Ručak

Utorak 18.10.2005.

I TEHNOLOGIJE I POSTROJENJA

16:00÷17:15	I.1 PRIJEMNA ISPITIVANJA SISTEMA AUTOMATSKOG REGULISANJA BROJA OBRTAJA ROTORA PARNIH TURBINA *Dragoljub Živković, Branislav Savić* I.2 NEKI REZULTATI RAZVOJA I PRETHODNOG ISPITIVANJA SOFTVERSKOG SISTEMA ZA DIJAGNOSTIKU RADA, EKONOMIČNOSTI I STANJA PARNOG BLOKA TERMOELEKTRANE *Branislav Savić, Vladimir Stevanović, Zoran Ribar, Radiša Jovanović, Milorad Dobrosavljević, Milenko Ranković* I.3 PROCENA PREOSTALOG RADNOG VEKA ELEMENTA TERMOELEKTRANE *M. Živković, G. Jovičić, S. Vulović, N. Đorđević* I.4 MOGUĆNOST PRIMENE GUSTE HIDROMEŠAVINE U TRANSPORTU I DEPONOVANJU PEPELA NA TERMOELEKTRANI "NIKOLA TESLA" – OBRENOVAC *Pavle Stjepanović, Dragan Dražović, Nebojša Kostović, Nenad Milojković* I.5 POSSIBILITIES FOR EFFICIENCY IMPROVEMENTS OF LIGNITE FIRED THERMO POWER PLANT WITH 225 MW *Vladimir I. Mijakovski* *PREZENTACIJA SPONZORA*
17:15÷17:30	***Kafe pauza***
17:30÷19:00	I.6 ODREĐIVANJE TOPLOTNOG EKVIVALENTA PROIZVODNE CENE ELEKTRIČNE ENERGIJE ZA TERMOELEKTRANE NA KOLUBARSKI LIGNIT *Jelenko B. Manić, Radmila D. Daničić* I.7 UTICAJ TEMPERATURE RASHLADNE VODE NA ENERGETSKU EFIKASNOST PARNOG BLOKA *Slobodan Laković, Mirjana Laković, Mladen Stojiljković* I.8 UTICAJ PROTOKA RASHLADNE VODE NA PERFORMANSE KONDENZATORA TERMOENERGETSKOG POSTROJENJA *Mirjana Laković, Slobodan Laković, Dejan Mitrović* I.9 THERMODINAMICAL APPROACH IN POWER PLANT OPTIMIZATION-CASE STUDY TE-TO ZRENJANIN *Predrag Rašković, Sreten Stoiljković, Miladin Čepić, Nenad Priljeva, Dragan Trtica* I.10 ULOGA TERMOELEKTRANE-TOPLANE U ENERGETSKOJ EFIKASNOSTI I EKOLOGIJI *Aleksa Marković, Ljubinka Marković, Miladin Čepić* I.11 HRSG TESTS, AS PART OF 2xST 18 POWER PLANT, BEFORE DELIVERY *Ene Barbu, Ioan Rosu, Tatiana Toma, George Turcu* I.12 DISTRIBUIRANA KOGENERACIJA - TEHNIČKA, EKONOMSKA ILI POLITIČKA PITANJA - *J. R. Petrović* *PREZENTACIJA SPONZORA*

Sreda 19.10.2005.	
	I TEHNOLOGIJE I POSTROJENJA
09:00÷10:30	I.13 UNAPREĐENJE RADIJACIONO-KONVEKTIVNE PEĆI NA ČVRSTO GORIVO *D. Stojiljković, V. Jovanović, M. Radovanović, N. Manić, I. Radulović, S. Perišić, D. Bećarević* I.14 IZBOR I ANALIZA EFIKASNIH POSTUPAKA SAGOREVANJA DOMAĆIH ULJNIH ŠKRILJACA *B. S. Repić, N. J. Đajić, B. D. Grubor* I.15 PRIMENA ADITIVA PRI SAGOREVANJU MAZUTA U PARNIM KOTLOVIMA *Slobodan Stevanović, Nada Tatalović* I.16 STANJE I PRAVCI DALJEG RAZVOJA SISTEMA DALJINSKOG GREJANJA (SCG) GRADA PIROTA *Dušan Ćirić, Đorđe Petrović, Velimir Stefanović* I.17 RAZVOJ UDALJENE TELEMETRIJSKE STANICE ZA PRAĆENJE ISPORUKE PRIRODNOG GASA GRADSKIM TOPLANAMA *Goran Krunić, Branislav Atlagić, Dragan Kukolj, Uroš Grbić* I.18 RAZVOJ UREĐAJA ZA PELETIRANJE PILJEVINE *D. Tucaković, T. Živanović, D. Stojiljković, V. Jovanović, B. Agbaba, I. Radulović, N. Manić* I.19 METODI DIJAGNOSTIKOVANJA ODVAJAČA KONDENZATA *Dušan Gordić, Milun Babić, Nebojša Jovičić, Vanja Šušteršić, Dubravka Jelić*
10:30÷10:45	***Kafe pauza***
10:45÷12:00	I.20 POSTROJENJE ZA DESALINIZACIJU SA KOMPRESIJOM PARE – MOGUĆNOSTI POVEĆANJA EFIKASNOSTI PROCESA OSTVARIVANJEM KAPLJIČASTE KONDENZACIJE *Nebojša Lukić, Alfred Leipertz, Andreas Fröba, Liv Diezel* I.21 PRIMENA EJEKTORA U PROIZVODNJI KOMPRIMOVANOG GASA – VAZDUHA *Aleksandar Petrović, Ljubomir Petrović, Aleksandar Dedić* I.22 TEHNIČKA REGULATIVA U GASNOM SEKTORU ZEMALJA JUGOISTOČNE EVROPE *Vojislav Vuletić* I.23 OPTIMIZACIJA SISTEMA ZA TEČNI NAFTNI GAS NA VOZILIMA ZASTAVE *Milan Milovanović, Stojan Petrović, Miliš Radisavljević, Saša Spasojević* I.24 SAVREMENE TEHNIKE ISPITIVANJA PARCIJALNOG PRAŽNJENJA U IZOLACIJI NAMOTAJA OBRTNIH MAŠINA *Dejan Rebrić, Dragan Petrović, Radovan Radosavljević, Siniša Stojković* *PREZENTACIJA SPONZORA*
12:00÷12:15	***Kafe pauza***
	II PROSTIRANJE TOPLOTE I MATERIJE. SAGOREVANJE
12:15÷14:00	II.1 REKONSTRUKCIJA RASHLADNOG TORNJA U CILJU POVEĆANJA EFIKASNOSTI HLAĐENJA *Dušan Golubović* II.2 KONVEKTIVNO PRELAŽENJE TOPLOTE PRI UDARU VAZDUŠNIH MLAZEVA U PREGRADU *Bogosav M. Vasiljević, Miloš J. Banjac* II.3 ODREĐIVANJE GUBITKA USLED SPOLJAŠNJEG HLAĐENJA KOTLOVA UCK-50 *Vladan Ivanović, Nenad Kažić, Dečan Ivanović* II.4 MERENJE KOEFICIJENTA PROLAZA TOPLOTE PROZORA *Velimir Stefanović, Mirko Stojiljković* II.5 MINIMALNA BRZINA FLUIDIZACIJE PRAŠKASTIH MATERIJALA U DVOKOMPONENTNOM FLUIDIZOVANOM SLOJU *Jelena Janevski, Branislav Stojanović, Mladen Stojiljković* II.6 UTICAJ MEHANIČKE AKTIVACIJE NA KVALITET CEMENTNIH MEŠAVINA KOJE SADRŽE LETEĆI PEPEO *Gordana Stefanović, Ljubica Ćojbašić, Ž. Sekulić* II.7 ODREDJIVANJE KOEFICIJENTA PRELAŽENJA VLAGE KOD SUŠENJA TERMO-DRVETA PREKO HEMIJSKOG POTENCIJALA PRENOSA *Aleksandar Dedić, Nenad Ćuprić, Duško Salemović* II.8 EKSPERIMENTALNO ODREDJIVANJE KOEFICIJENTA PROLAZA TOPLOTE KROZ ZAGREVNE POVRŠINE PLOČASTOG UPARIVAČA U FABRICI ŠEĆERA ŠAJKAŠKA – ŽABALJ *Jasna Grbić, Zoltan Zavargo, Aleksandar Jokić, Rada Jevtić-Mučibabić, Nikola Dokmanović* II.9 SAGORIJEVANjE LIGNITA STANARI *Vinko Babić* *PREZENTACIJA SPONZORA*
14:00÷16:00	**Ručak**

Sreda 19.10.2005.	
	III ENERGETSKA EFIKASNOST
16:00÷17:15	III.1 UPOTREBA TERMOVIZIJE I ODREĐIVANJE INFILTARACIONIH GUBITAKA KAO SREDSTAVA ZA OCENU ENERGETSKIH GUBITAKA U STAMBENIM ZGRADAMA *Dragoslav Šumarac, Maja Đurović-Petrović, Stanko Ćorić* III.2 MERENJA TEMPERATURE, RELATIVNE VLAŽNOSTI, TOPLOTNOG FLUKSA I POTROŠENE TOPLOTNE ENERGIJE *Veljko Georgijević, Miloš Anđelković* III.3 UTICAJ GRADNJE OBJEKATA NA IZBOR PARAMETARA SOBNOG TERMOSTATA *Pavle Kaluđerčić, Novak Prodanović* III.4 POVEĆANJE EFIKASNOSTI SISTEMA CENTRALNOG GREJANJA REGULACIJOM I MERENJEM UTROŠENE TOPLOTNE ENERGIJE *Branislav Stojanović, Jelena Janevski* III.5 SAVREMENE ENERGETSKI EFIKASNE PROZORSKE KONSTRUKCIJE *Dragan Gavrilović, Velimir Stefanović* III.6 ENERGYEFFICENCY IN THE BUILDING ENERGETICS – research case - *Tatiana V. Toma* III.7 MOGUĆNOSTI REKUPERACIJE TOPLOTE PRI ZAGREVANJU BAZENA *Mirko M. Stojiljković, Bratislav D. Blagojević, Mladen M. Stojiljković, Marko G. Ignjatović* III.8 REKUPERATIVNI IZMENJIVAČI TOPLOTE I ANALIZA POVEĆANJA ENERGETSKE EFIKASNOSTI U KLIMA-VENTILACIONIM KOMORAMA *Dejan Petrović, Gradimir Ilić* *PREZENTACIJA SPONZORA*
17:15÷17:30	***Kafe pauza***
17:30÷19:00	III.9 RACIONALIZACIJA POTROŠNJE ENERGIJE U FABRICI AUTO-GUMA TRAYAL KORPORACIJE U KRUŠEVCU *Slađana Živadinović, Miroslav Savić* III.10 PRELIMIBARNI ENERGETSKI BILANS KOTLOVSKOG POSTROJENJA U FABRICI TIGAR MH-BABUŠNICA *Mladen Stojiljković, Dejan Mitrović, Goran Vučković, Danijela Tošić* III.11 GAZDOVANJE ENERGIJOM U FABRICI TIGAR MH U BABUŠNICI *Goran Vučković, Mladen Stojiljković, Dejan Mitrović, Mića Vukić* III.12 ENERGETSKA EFIKASNOST U SISTEMIMA ZA DISTRIBUCIJU PARE I POVRAĆAJ KONDENZATA U AD PIVARA NIŠ *Dejan Mitrović, Mladen Stojiljković, Goran Vučković, Mirko Stojiljković* III.13 FINE COAL PELLETIZING CONTRIBUTION TO ENERGY EFFICIENCY *Vojin Čokorilo, Dinko Knezević, Vladimir Milisavljević* III.14 ENERGY SAVINGS OF A WATER PUMP WITH VFD IN AIR CONDITIONING SYSTEMS *Vladimir I. Mijakovski, Kire J. Popovski* III.15 OZNAČAVANjE ENEGETSKE EFIKASNOSTI PUTNIČKIH VOZILA U EVROPI *S. Petrović, M. Tomić* III.16 KOMBINOVANI TRANSPORT U FUNKCIJI ENERGETSKE EFIKASNOSTI *Anica Milošević, Dušan Stamenković, Miloš Milošević* *PREZENTACIJA SPONZORA*

Četvrtak 20.10.2005.	
	IV NOVI I OBNOVLJIVI IZVORI
09:00÷10:30	IV.1 RAZVOJ HIBRIDNOG RAVNOG SOLARNOG PRIJEMNIKA *M. Bojić, M. Despotović* IV.2 TOPLOTNA EFIKASNOST HIBRIDNOG I OBIČNOG RAVNOG SOLARNOG PRIJEMNIKA U ZAVISNOSTI OD NJIHOVIH KONSTRUKCIJSKIH PARAMETARA *M. Bojić, V. Šušterčić, R. Janković* IV.3 PRIMER SOLARNOG PRIJEMNIKA ZA SREDNJETEMPERATURNU KONVERZIJU SUNČEVOG ZRAČENJA U TOPLOTU *Boban Nikolić, Velimir Stefanović* IV.4 RAZMATRANJE MOGUĆNOSTI KORIŠĆENJA SUNČEVE ENERGIJE NA PRIMERU TO “CERAK” *N. B. Miloradović* IV.5 PRIKAZ REŠENJA POKRETNE UNIVERZALNE SOLARNE SUŠARE ZA SUŠENJE BIOLOŠKIH METERIJALA *Radivoje M. Topić, Aleksandar Lj. Petrović, Nenad Lj. Ćuprić* IV.6 METODOLOGIJA PROCENE ENERGIJE VETRA NA MEZO/MIKRO LOKACIJAMA *Žarko Stevanović, Predrag Živković, Maja Studović* IV.7 OPTIMALNO PROJEKTOVANJA FARMI VJETROELEKTRANA *E. Zlomušica, M. Behmen, F. Ćatović, K. Šehbajraktarević* *PREZENTACIJA SPONZORA*
10:30÷10:45	***Kafe pauza***
10:45÷12:00	IV.8 MOGUĆNOSTI I OPRAVDANOST KORIŠĆENJA GEOTERMALNE BUŠOTINE U BEČEJU *J. R. Petrović, M. P. Marić, Đ. S. Bašić* IV.9 MOGUĆNOST KORIŠĆENJA GEOTERMALNE ENERGIJE SOKOBANJE *Predrag Milanović, Vojislav Tomić* IV.10 IDENTIFIKACIJA GEOMETRIJE I MASE OBRTNOG KOLA MALE HIDROTURBINE *Nikola L. Maričić* IV.11 BANKI TURBINA – POGODAN TIP MALE HIDROTURBINE ZA ISKORIŠĆENJE POTENCIJALA MALIH REKA (TOKOVA) *Branislav Ignjatović, Miroslav Benišek, Miloš Nedeljković, Dejan Ilić, Đorđe Čantrak, Ivan Božić* IV.12 BIOMASS AS ENERGY SOURCE IN LOCAL CONDITIONS IN MACEDONIA *Ilija J. Petrovski, Risto V. Filkoski* *PREZENTACIJA SPONZORA*
12:00÷12:15	***Kafe pauza***
12:15÷14:00	IV.13 SAGORJEVANJE MJEŠAVINA UGLJEVA I BIOMASE KAO MOGUĆNOST REDUKCIJE EMISIJE SUMPORNIH OKSIDA *P. M. Gvero, D. Stojiljković, Đ. Vojinović, G. Tica, S. Đukić* IV.14 BIOGAS KAO ENERGETSKI IZVOR *Gordana Tica, Petar Gvero, Slaviša Jelisić, Dragoslava Stojiljković* IV.15 KRITIČKA ANALIZA DOSADAŠNJIH RJEŠENJA PROBLEMA DRVNOG OTPADA I IZBOR OPTIMALNE TEHNOLOGIJE ZA PRERADU OTPADNE DRVNE BIOMASE *M. Tica, V. Miltenović, M. Djurdjević* IV.16 PRELIMINARNI REZULTATI ISPITIVANJA EKSPERIMENTALNOG POSTROJENJA SNAGE 2 MW NA BALE SOJINE SLAME *R. Mladenović, D. Dakić, A. Erić, M. Mladenović, B. Repić, M. Paprika* IV.17 KORIŠĆENJE BIOGASA NA FARMI *Saša Igić, Miloš Milanković, Igor Srejić, Dragoslav Perić* IV.18 MISCANTHUS GIGANTEUS - OSNOVA NOVOG BIOENERGETSKOG GORIVA *G. Dražić, N. Mihailović, Ž. Dželetović, B. Stevanović, J. Šinžar* *PREZENTACIJA SPONZORA*
14:00÷16:00	**Ručak**

Četvrtak 20.10.2005.	
V MATEMATIČKO MODELIRANJE I NUMERIČKE SIMULACIJE	
16:00÷17:15	V.1 INTEROPERABILNOST SOFTVERA ZA ODRŽIVE ZGRADE *M. Bojić, M. Todorović* V.2 KONCEPCIJA RAČUNARSKI PODRŽANOG NADZORNO-UPRAVLJAČKOG SISTEMA KOMPLEKSA ZA ODVODNJAVANJE POVRŠINSKOG KOPA UGLJA "DRMNO" *Slobodan Vujić, Toma Tanasković, Žarko Krstić, Lazar Cvetković, Aleksandar Petrovski, Igor Miljanović* V.3 RAZVOJ PREDIKTORA ISPORUKE PRIRODNOG GASA U SISTEMU NIS-GAS *Adnan H. Hodžić, Dragan D. Kukolj, Branislav S. Atlagić, Miroslava Lj. Dražić* V.4 PROGRAMSKA APLIKACIJA ZA ANALIZU INDUSTRIJSKIH KOMPRESORSKIH RASHLADNIH POSTROJENJA *D. Gvozdenac, M. Kljajić* V.5 UTICAJ NESTACIONARNOG TRENJA KOD PRELAZNIH PROCESA U HIDRAULIČKIM CIJEVNIM SISTEMIMA *Uroš Karadžić, Anton Bergant, Igor Vušanović* *PREZENTACIJA SPONZORA*
17:15÷17:30	***Kafe pauza***
17:30÷19:00	V.6 MATEMATIČKA SIMULACIJA RADA MREŽE NAVODNJAVANJA KIŠENJEM *Božidar Bogdanović, Jasmina Bogdanović-Jovanović, Saša Milanović* V.7 MATEMATIČKI MODEL I NUMERIČKA SIMULACIJA PROCESA PROIZVODNJE U FABRICI AUTO GUMA TRAJAL KORPORACIJE U KRUŠEVCU *Slađana Živadinović* V.8 PRIMENA MONTE-KARLO SIMULACIJE U ANALIZI POUZDANOSTI SISTEMA *Dragan Milčić, Miroslav Mijajlović* V.9 THE SYSTEM OF UNIVERSAL EQUATIONS OF UNSTEADY MHD INCOMPRESSIBLE FLUID FLOW WITH VARIABLE ELECTRO CONDUCTIVITY ON HEATED MOVING POROUS PLATE *Zoran Boričić, Dragiša Nikodijević, Dragica Milenković, Živojin Stamenković* V.10 PRIMENA MATLAB® OKRUŽENJA ZA TERMIČKI PRORAČUN TOPLOVODNOG KOTLA ZA SAGOREVANJE DRVENIH PELETA *B. Stojanović, M. Protić, B. Blagojević , J. Janevski, M. Ignjatović* V.11 NUMERIČKA SIMULACIJA PROCESA U RAZLIČITIM GEOMETRIJAMA KANALA ZA AEROSMEŠU SA PLAZMENIM SISTEMOM POTPALE *M. A. Sijerčić, S. V. Belošević, P. Lj. Stefanović* V.12 NUMERIČKA SIMULACIJA RASPODELE UGLJENOG PRAHA DUŽ KANALA AEROSMEŠE U ZAVISNOSTI OD POLOŽAJA USMERAVAJUĆIH LOPATICA *Nikola V. Živković, Goran S. Živković, Predrag Lj. Stefanović* V.13 PARAMETARSKA ANALIZA STRUJANJA VAZDUHA KROZ KANAL AEROSMEŠE GORIONIČKOG PAKETA *Zoran J. Marković, Predrag Lj. Stefanović, Dejan B. Cvetinović,* *Zoran N. Pavlović, Nikola V. Živković, Milijana J. Paprika* *PREZENTACIJA SPONZORA*
20:00÷	***Svečana večera***

Petak 21.10.2005.	
	V MATEMATIČKO MODELIRANJE I NUMERIČKE SIMULACIJE
09:00÷10:15	V.14 LES TURBULENTNOG STRUJANJA U KANALU *Zoran Pavlović, Satoru Komori* V.15 UTICAJ GRANIČNIH USLOVA NA MODELIRANJE STRUJNO TERMIČKIH PROCESA U HORIZONTALNOM ISPARIVAČU *M. Pezo, Ž. Stevanović, V. Stevanović* V.16 NUMERIČKA SIMULACIJA PRENOŠENJA TOPLOTE I PADA PRITISKA U KANALIMA IZMEĐU PARALELNIH PROFILISANIH PLOČA *Mirko Dobrnjac, Gradimir Ilić, Žarko Stevanović, Valentina Turanjanin* V.17 CFD ANALIZA 3D KOMPLEKSNOG TURBULENTNOG STRUJANJA VAZDUHA U KOMORI ZA TALOŽENJE KAMENE VUNE *Predrag Živković, Gradimir Ilić, Žarko Stevanović, Mića Vukić, Dragan Gavrilović, Branislav Antić* V.18 SIMULACIJA TERMO-STRUJNIH PROCESA NA LOKALNOM NIVOU U DOBOŠASTIM IZMENJIVAČIMA TOPLOTE *Mića Vukić, Predrag Živković, Goran Vučković, Nenad Radojković, Gradimir Ilić, Žarko Stevanović* V.19 NUMERIČKA SIMULACIJA PRENOSA TOPLOTE U RENDGEN CEVI *Mića Vukić, Predrag Živković, Goran Vučković, Nenad Radojković, Gradimir Ilić, Žarko Stevanović* V.20 MATEMATIČKI MODEL PIROLIZE ČVRSTE MATERIJE *B. Miljković, B. Stepanov, I. Pešenjanski*
10:15÷10:30	***Kafe pauza***
	VI ZAŠTITA ŽIVOTNE SREDINE
10:30÷12:00	VI.1 OBAVEZE SRBIJE I CRNE GORE U OBLASTI ENERGETIKE, PREMA ATINSKOM MEMORANDUMU I KJOTO PROTOKOLU, RADI OČUVANJA I UNAPREĐENJA ŽIVOTNE SREDINE *Miloš Tešić, Miodrag Mesarović* VI.2 UTICAJ TERMOENERGETSKIH OBJEKATA NA KVALITET VAZDUHA *G. H. Kanevče, Lj. P. Kanevče* VI.3 MOGUĆNOST SMANJENJA EMISIJE OKSIDA AZOTA PRIMENOM VIHORNOG GORIONIKA *Miroljub M. Adžić, Marija A. Živković,Aleksandar M. Milivojević* VI.4 PROBLEM EMISIJE FINIH ČESTICA DIZEL MOTORA *Velimir S. Petrović, Srećko Grojić, Đuro Borak* VI.5 ENERGETSKI I EKOLOŠKI EFEKTI SUPSTITUCIJE KONVENCIONALNIH GORIVA BIOBRIKETIMA *Ivan M. Mijailović* VI.6 PRIMER IZBORA HIDROMAŠINSKE OPREME STANICE ZA PREČIŠĆAVANJE OTPADNIH VODA TIPA SBR *S. Panovski, G. Janevska* VI.7 MOGUĆNOSTI ISKORIŠĆENJA ENERGIJE IZ GRADSKOG OTPADA *N. Jovičić, M. Babić, D. Gordić, D. Jelić, V. Šušteršič* VI.8 ISPITIVANJE KOLIČINE I SASTAVA ČVRSTOG OTPADA *Gordana Stefanović, Lj. Ćojbašić, P. Stošić, M. Nikolić, D. Marković* VI.9 SOCIJALNO-EKONOMSKI ASPEKTI REKULTIVACIJE ODLAGALIŠTA POVRŠINSKIH KOPOVA UGLJA U FAZI RESTRUKTUIRANJA EPS-a *Slobodan Vujić, Svetozar Kovačević, Aleksandra Čanak-Nedić, Igor Miljanović, Aleksandar Petrovski*
12:00÷13:00	***Skupština Društva termičara***
13:00	***Zatvaranje simpozijuma***

MECHANICAL VAPOR COMPRESSION DESALINATION PLANT – EFFICIENCY INCREASING POSSIBILITIES OF PROCESS USING DROPWISE CONDENSATION

Dr Nebojša Lukić, vanr.prof.
Mašinski fakultet u Kragujevcu
Prof.Dr.-Ing Alfred Leipertz, Dr.-Ing Andreas Fröba, Dipl.Ing. Liv Diezel
Department Engineering Thermodynamics, Friedrich-Alexander University, Erlangen-Nürnberg, Germany

Abstract

Using ion-implanted metallic surfaces to provoke a dropwise condensation improves a convective heat transfer coefficient significantly. Thermal desalination process, especially mechanical vapor compression (MVC) could be more effective by ion-implantation technology. This paper points on a possible heat transfer area reduction using defined approach. In defined MVC plant simulation model (mathematical model and realized software), a replacing filmwise by dropwise condensation can improve both main convective heat transfer process (condensation and evaporation) by arising a condensation heat transfer coefficient and also a heat flux value (respectively). For assumed improvement factor of dropwise condensation, comparing with filmwise condensation by the same MVC plant capacity, the reduction of main heat exchanger area is within 40% and 45%.

1. Introduction

Despite a huge amount of water that we are surrounded, a drinking water shortage becomes the world problem. Whence the biggest part of this amount is saline water, one of logical solution is desalination. There are two main desalination techniques: membrane and evaporation. In other words, we can use non-thermal or thermal process to obtain drinking water. Membrane technique as reverse osmosis (RO) is generally a low energy and low price but also low product quality desalination method.

Point of our interest is evaporation technique. Depends on desalination plant capacity, availability of steam sources, electrical energy prices and specific demands, different thermal process can be used. Those are mainly: Multi-Stage Flash distillation (MSF), Multi Effect Distillation (MED), Thermal and Mechanical Vapor Compression (TVC and MVC) [1]. Thermal techniques that require an external steam source (MSF, MED, TVC) can be improved by cogeneration process [5]. Because an evaporation of saline (sea) water is obligatory for defined techniques, a problem of energy efficiency is dominant. In other words the condensation latent heat of product water should be used to provoke evaporation of saline water in condition when the temperature level of produced vapor is not enough to enable stabile evaporation of saline water. Recovering energy ratio of mechanical vapor compression (MVC) technique (vapor is pressurized by compressor) can be very high but a spent energy is very expensive electrical energy. This is one stage desalination method for smaller product capacities (up to 3000 m^3/day). In MVC plants, rang of the specific energy consumption is mostly 7-12 kWh/m^3. Higher energy efficiency means a smaller evaporation-condensation side temperature difference and bigger demanded heat transfer area. There is chance for scientists to achieve an optimum thermal desalination scenario.

Many approaches to mentioned scenario are recorded. In [2], the realized MVC desalination plants have given a good production results but because small evaporation-condensation side temperature difference (dt=3-4°C) the used plate one-phase and tube evaporation-condensation heat exchangers are huge (heat transfer area of he_{ec}=2598 m^2). In [3] the classic MVC model was considered by simple LMTD calculation method for heat transfer phenomena. In Vapor compression plant (VC), a dominant centrifugal compressor and its significant consumption of electrical energy can be replaced by classic heat pump cycle [7], [4], [6], absorption heat pump cycle [4], thermal vapor compression (TVC), using ejector and external steam source [4].

Farther, in heat pump cycle energy consumption can be reduced using solar energy for working fluid evaporation (delimited from water cycle) [6]. All mentioned desalination plant model or installation decrease specific energy consumption (exception is TVC) very effective but problem is its limited production capacity often on insufficient level. On other side a centrifugal compressor can be driven by wind energy [8], [9] but beside small production capacity, a stabile plant functioning is basic problem of this concept. The aim of all presented methods is energy efficiency increasing by reduction of MVC demanded driving electrical energy.

Other (our) approach is based on improvement of MVC plant heat transfer coefficient. Plate heat exchanger (PHE) concept provides high heat transfer coefficient (very low turbulent transition Re number) and relative small pressure drop for any heat transfer scenario (one-phase, evaporation, condensation) [10]. On other side filmwise condensation (FWC) can be converted to more effective dropwise condensation (DWC) using ion implanted metallic surface. This means significant multiplied condensation heat transfer coefficient depending on heat transfer conditions [12], [13]. Probably, using on the same way treated metallic surface, it can also improve evaporation heat transfer coefficient but it needs more investigation. In [11] it was described the successful inhibition of scaling process in desalination plant using ion implanted metallic surface but there same improvement of evaporation heat transfer coefficient can be found. Further it will be presented the designed MVC mathematical model (based on PHE and DWC) and the obtained results.

2. MVC Mathematical model

2.1 *The assumed desalination plant*

The assumed mechanical vapor compression desalination plant (MVC) is consisted of two one-phase plate heat exchangers (parallel connection) and one main evaporation-condensation plate heat exchanger and other necessary equipments. The schematic diagram of MVC one-phase he parallel connection is shown on figure 2.1

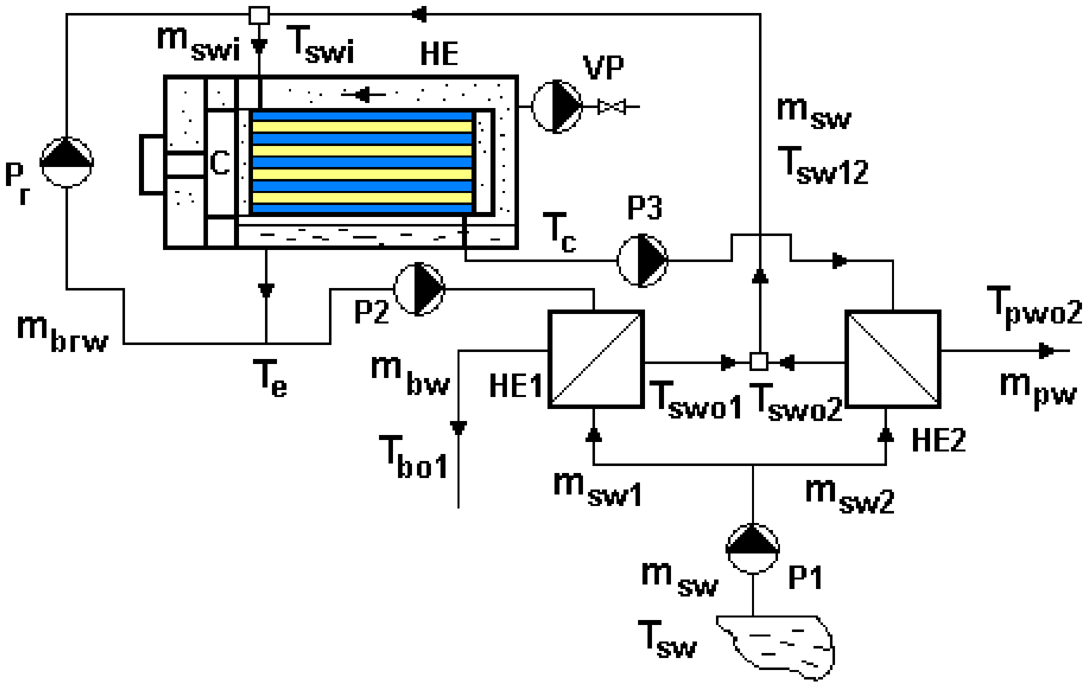

Figure 1.1 Schematic diagram of the MVC desalination plant

There are:

HE1 - the brine heat exchanger,
HE2 - the product water heat exchanger,
HE - the main (evaporation-condensation) heat exchanger,
P1,P2,P3,P_r - pumps,
VP - vacuum pump,
C - compressor,
m_{pw} - product water mass flow rate (kg/s);
m_{sw} - sea water mass flow rate (kg/s);
m_{bw} - brine mass flow rate (kg/s);
m_{bwr} - recirculation brine mass flow rate (kg/s);
m_{sw1} - sea water mass flow rate throughout HE1 (kg/s);
m_{sw2} - sea water mass flow rate throughout HE2 (kg/s);
m_{swi} - sea water mass flow rate throughout main heat exchanger (HE) (kg/s);
t_{sw} - temperature of environmental sea water (^oC);
t_e - evaporation temperature (^oC);
t_c - condensation temperature (^oC);
t_{bo1} - HE1 outlet temperature of brine (^oC);
t_{pwo2} - HE2 outlet temperature of product water (^oC);
t_{swo1} - HE1 outlet temperature of sea water (^oC);
t_{swo2} - HE2 outlet temperature of sea water (^oC);

t_{swi} - HE inlet temperature of sea water (^oC);
t_{swo12} - outlet temperature of sea water after mixing HE1 and HE2 flows (^oC).

During real functioning of MVC plant, instead the water evaporation temperature, t_e (^oC), the increased saline water evaporation temperature, t_{be} (^oC) exists. This temperature is function of pure water evaporation temperature and salt percent s_{p100} (%) or salt ratio s_p (-), $t_{be}=f(te,s_{p100})$.

2 *The one-phase plate heat exchanger mathematical model*

According to the shown picture 1.1 (he parallel connection), mass and energy equations, the one-phase parallel connection mathematical model can be expressed. Convective heat transfer coefficients of one-phase plate heat exchangers HE1 and HE2 are calculated according to [14]. Warm outlet flows of brine and product water from HE1 and HE2 present the MVC plant heat losses:

$$Q_{l1}=m_{bw}\cdot c_{bw}\cdot(t_{bo1}-t_{sw}) \ , \qquad (2.31)$$

$$Q_{l2}=m_{pw}\cdot c_{w}\cdot(t_{pwo2}-t_{sw}) \ . \qquad (2.32)$$

There are:
Q_{l1} - heat loss of heat exchanger HE1 (kW);
Q_{l2} - heat loss of heat exchanger HE2 (kW).

The MVC heat losses must be equal with MVC heat gain, the real compressor power, P_{rc} (kW):

$$P_{rc}=Q_{l1}+Q_{l2} \ , \qquad (2.33)$$

and according to this equation, the one-phase heat transfer areas of HE1 and HE2 should be adjusted (changing of N_{o1},N_{o2},w_1,w_2,h_1,h_2) to real values.

3 *The evaporation-condensation plate heat exchanger (HE_m) mathematical model*

The real compressor power is calculated as:

$$l_{tcr}=\frac{h_{cisv}-h_{ebsv}}{\eta_{ic}}; \quad P_{rc}=m_{pw}\cdot l_{tcr} \ . \qquad (3.1)$$

There are:
l_{tcr} - compressor real technical work (kJ/kg);
h_{ebsv} - compressor inlet vapor enthalpy, superheated vapor enthalpy, $h_{ebsv}=f(p_e,t_{be})$ at water evaporation pressure p_e (MPa)=f(t_e) and saline water evaporation temperature t_{be} ($t_{be}>t_e$) (kJ/kg). This enthalpy is bigger than saturated vapor enthalpy at temperature t_e.;
h_{cisv} - isentropic compressor outlet vapor enthalpy, superheated vapor enthalpy, $h_{cisv}=f(p_c,s_{ebsv})$ at water condensation pressure p_c (MPa)=f(t_c) and superheated vapor entropy, $s_{ebsv}=f(p_e,t_{be})$ (kJ/kg);
η_{ic} - isentropic compressor efficiency (assumed value) (-).

The real compressor outlet vapor enthalpy is calculated as:

$$h_{crsv} = h_{ebsv} + P_{rc} \quad . \tag{3.2}$$

The compressor outlet vapor temperature t_{crsv} (^oC)=f(p_c,h_{crsv}) is function of condensation pressure, p_c and real compressor outlet vapor enthalpy, h_{crsv}. For computer calculation of saturated and superheated vapor properties, the high precise equations are used.

The specific compressor energy consumption (≈MVC energy consumption), E_{sc} (kwh/m^3) per m^3 of product water is calculated as:

$$E_{sc} = \frac{24 \cdot P_{rc}}{Q_{MVC}} \quad . \tag{3.3}$$

There is:
Q_{MVC} - capacity of MVC plant (m^3/day).

The efficiency factor of MVC plant, F_e (-) is calculated as:

$$F_e = \frac{r_{te}}{l_{tcr}} \quad . \tag{3.4}$$

There is:
r_{te} - water evaporation latent heat at evaporation pressure (kJ/kg).

Two stream cases are possible in HE_m:
- parallel flow HE_m;
- counter flow HE_m.

The parallel flow HE_m has three possible heat transfer zones (Fig. 3.1 and 3.2):
- vapor-brine heat transfer zone (HE_m inlet);
- vapor-evaporation heat transfer zone or brine-condensation heat transfer zone;
- evaporation-condensation heat transfer zone (main heat transfer area).

Figure 3.1 Schematic diagram of parallel flow HE_m, case $Q_{vbc}>Q_{wae}$

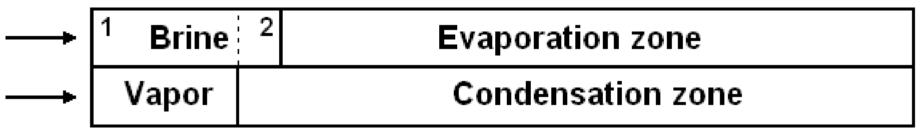

Figure 3.2 Schematic diagram of parallel flow HE_m, case $Q_{vbc}<Q_{wae}$

There Q_{vbc} (kW) presents the heat power needed to achieve the saturated vapor state (vapor cooling to start of condensation) and Q_{wae} (kW) presents the heat power needed to achieve the saturated brine liquid state (brine heating to start of evaporation). The heat power Q_{vbc} and Q_{wae} are calculated as:

$$Q_{wae} = m_{swi} \cdot c_{bw} \cdot (t_{be} - t_{swi}) \ , \tag{3.5}$$

$$Q_{vbc} = m_{pw} \cdot (h_{crsv} - h_c) \ . \tag{3.6}$$

There is h_c - saturated enthalpy at condensation temperature (kJ/kg).

The counter flow HE_m has three possible heat transfer zones (Fig. 3.3):
- vapor-evaporation heat transfer zone (HE_m inlet);
- brine-condensation heat transfer zone (HE_m outlet);
- evaporation-condensation heat transfer zone (main heat transfer area).

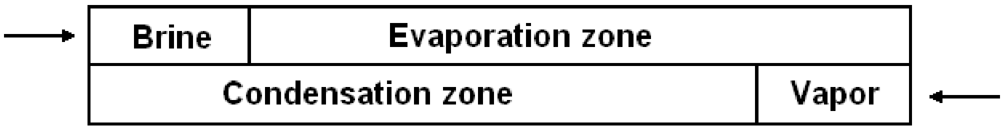

Figure 3.3 Schematic diagram of counter flow HE_m

The real HE_m inlet temperature of sea water, t_{swi} is calculated using the heat power equality of HE_m evaporation and condensation side:

$$m_{swi} \cdot c_{bw} \cdot (t_{be} - t_{swi}) + m_{pw} \cdot r_{te} = m_{pw} \cdot (h_{crsv} - h_c) + m_{pw} \cdot r_{tc} \quad \Rightarrow$$

$$t_{swi} = t_{be} - m_{pw} \cdot (h_{crsv} - h_c + r_{tc} - r_{te}) / (m_{swi} \cdot c_{bw}) \tag{3.7}$$

There is r_{tc} - water condensation latent heat at condensation pressure (kJ/kg). According to the real temperature, tswi, the one-phase heat exchanger areas should be adjusted.

The heat transfer equations in HEm are:

$$Q_{hem} = A_{hem} \cdot U_{hem} \cdot \Delta t_{mm} ; Q_{hem1} = A_{hem1} \cdot U_{hem1} \cdot \Delta t_{mm1} ; Q_{hem2} = A_{hem2} \cdot U_{hem2} \cdot \Delta t_{mm2} \tag{3.8}$$

There are:
Q_{hem} - heat power of evaporation-condensation HE_m area (kW);
Q_{hem1} - heat power of inlet HE_m area (kW);
Q_{hem2} - heat power of outlet (or second inlet) HE_m area (kW);
A_{hem} - heat transfer area of evaporation-condensation HE_m zone (m^2);
A_{hem1} - heat transfer area of inlet HE_m zone (m^2);
A_{hem2} - heat transfer area of outlet (or second inlet) HE_m zone (m^2);
U_{hem} - total heat transfer coefficient of evaporation-condensation HE_m area (W/m^2K);
U_{hem1} - total heat transfer coefficient of inlet HE_m area (W/m^2K);
U_{hem2} - total heat transfer coefficient of outlet (or second inlet) HE_m area (W/m^2K);
Δt_{mm} - mean logarithmic tem. difference of evaporation-condensation HE_m area (^oC);
Δt_{mm1} - mean logarithmic temperature difference of inlet HE_m area (^oC);
Δt_{mm2} - mean logarithmic tem. difference of outlet (or second inlet) HE_m area (^oC).

According to figures 3.1-3.3 the mentioned heat powers are:

$$Q_{hem} = m_{pw} \cdot r_{tc} \quad \Rightarrow parallel \quad flow \Rightarrow Q_{vbc} \geq Q_{wae};$$
$$Q_{hem} = m_{pw} \cdot r_{tc} - (Q_{wae} - Q_{vbc}) \quad \Rightarrow parallel \quad flow \Rightarrow Q_{vbc} \leq Q_{wae}; \qquad (3.9)$$
$$Q_{hem} = m_{pw} \cdot r_{tc} - Q_{wae} \quad \Rightarrow counter \quad flow,$$

$$Q_{hem1} = Q_{wae} \quad \Rightarrow parallel \quad flow \Rightarrow Q_{vbc} \geq Q_{wae};$$
$$Q_{hem1} = Q_{vbc} \quad \Rightarrow parallel \quad flow \Rightarrow Q_{vbc} \leq Q_{wae}; \qquad (3.10)$$
$$Q_{hem1} = Q_{wae} \quad \Rightarrow counter \quad flow,$$

$$Q_{hem2} = Q_{vbc} - Q_{wae} \quad \Rightarrow parallel \quad flow \Rightarrow Q_{vbc} \geq Q_{wae};$$
$$Q_{hem2} = Q_{wae} - Q_{vbc} \quad \Rightarrow parallel \quad flow \Rightarrow Q_{vbc} \leq Q_{wae}; \qquad (3.11)$$
$$Q_{hem2} = Q_{vbc} \quad \Rightarrow counter \quad flow,$$

According to equation (3.8) the mean logarithmic temperature differences are:

$$\Delta t_{mm} = t_c - t_{be} \quad \Rightarrow for \quad all \quad three \quad cases \;, \qquad (3.12)$$

$$\Delta t_{mm1} = \frac{(t_{crsv} - t_{swi}) - (t_{sv} - t_{be})}{\ln(\frac{t_{crsv} - t_{swi}}{t_{sv} - t_{be}})} \quad \Rightarrow parallel \quad flow \Rightarrow Q_{vbc} \geq Q_{wae};$$
$$\Delta t_{mm1} = \frac{(t_{crsv} - t_{swi}) - (t_c - t_{wee})}{\ln(\frac{t_{crsv} - t_{swi}}{t_c - t_{wee}})} \quad \Rightarrow parallel \quad flow \Rightarrow Q_{vbc} \leq Q_{wae}; \qquad (3.13)$$
$$\Delta t_{mm1} = \frac{(t_c - t_{swi}) - (t_c - t_{be})}{\ln(\frac{t_c - t_{swi}}{t_c - t_{be}})} \quad \Rightarrow counter \quad flow.$$

$$\Delta t_{mm2} = \frac{(t_{sv} - t_{be}) - (t_c - t_{be})}{\ln(\frac{t_{sv} - t_{be}}{t_c - t_{be}})} \Rightarrow parallel \quad flow \Rightarrow Q_{vbc} \geq Q_{wae};$$

$$\Delta t_{mm2} = \frac{(t_c - t_{wee}) - (t_c - t_{be})}{\ln(\frac{t_c - t_{wee}}{t_c - t_{be}})} \Rightarrow parallel \quad flow \Rightarrow Q_{vbc} \leq Q_{wae}; \ , \qquad (3.14)$$

$$\Delta t_{mm2} = \frac{(t_{crsv} - t_{be}) - (t_c - t_{be})}{\ln(\frac{t_{crsv} - t_{be}}{t_c - t_{be}})} \Rightarrow counter \quad flow,$$

There are:
t_{sv} - superheated vapor temperature at point of saline water evaporation temperature, t_{be} achievement. Temperature t_{sv} (^oC)=f(p_c,h_{sv}) is function of condensation pressure, p_c and superheated vapor enthalpy at mentioned point, h_{sv}(kJ/kg)=h_{crsv}-Q_{wae}/m_{pw}, (^oC);
t_{wee} - brine temperature at point of product water condensation temperature, t_c achievement, $t_{wee}=t_{swi}+Q_{vbc}/(c_{bw}\cdot m_{swi})$ (^oC).

According to equation (3.8) the total heat transfer coefficients are:

$$U_{hem} = \frac{1}{\frac{1}{if_e \cdot h_{mevp}} + \frac{\delta_m}{\lambda_m} + \frac{1}{if_c \cdot h_{mcon}}} \Rightarrow all \quad three \quad cases, \qquad (3.15)$$

$$U_{hem1} = \frac{1}{\frac{1}{h_{1mw}} + \frac{\delta_m}{\lambda_m} + \frac{1}{h_{2mv}}} \Rightarrow \quad both \quad parallel \quad flow \quad cases;$$

$$U_{hem1} = \frac{1}{\frac{1}{h_{1mw}} + \frac{\delta_m}{\lambda_m} + \frac{1}{if_c \cdot h_{mcon}}} \Rightarrow counter \quad flow, \qquad (3.16)$$

$$U_{hem2} = \frac{1}{\frac{1}{if_e \cdot h_{mevp}} + \frac{\delta_m}{\lambda_m} + \frac{1}{h_{2mv}}} \Rightarrow parallel \quad flow \Rightarrow Q_{vbc} \geq Q_{wae};$$

$$U_{hem2} = \frac{1}{\frac{1}{h_{1mw}} + \frac{\delta_m}{\lambda_m} + \frac{1}{if_c \cdot h_{mcon}}} \Rightarrow parallel \quad flow \Rightarrow Q_{vbc} \leq Q_{wae}; \qquad (3.17)$$

$$U_{hem2} = \frac{1}{\frac{1}{if_e \cdot h_{mevp}} + \frac{\delta_m}{\lambda_m} + \frac{1}{h_{2mv}}} \Rightarrow counter \quad flow.$$

There are:
h_{mevp} - evaporation heat transfer coefficient in HE_m (W/m^{2}K);

h_{mcon} - condensation heat transfer coefficient in HE_m (W/m^2K);
h_{1mw} - convective heat transfer coefficient of brine in HE_m (W/m^2K);
h_{2mv} - convective heat transfer coefficient of superheated vapor in HE_m (W/m^2K);
δ_m - thickness of HE_m plate (m);
λ_m - thermal conductivity of HE_m plate (W/mK);
if_e - improvement factor of dropwise evaporation (-);
if_c - improvement factor of dropwise condensation (-).

The choosing of appropriate equations for condensation and evaporation heat transfer coefficient calculation in small channels as PHE flow area is very difficult problem. For example, in [22] can be found that eleven correlations for conventional and narrow-channel boiling predicted the data poorly, ranging form 250% average over-prediction to 70% average under-prediction. In [15]-[19], [23], can be fount more evaporation predictions of water and refrigerants in small pipe and PHE. Also, in [20], [21], [24] can be found condensation predictions of water and refrigerants in small pipe and PHE. According to assumed MVC mathematical model and presented literature, in further text, the most appropriate evaporation and condensation equations are assumed.

The condensation heat transfer coefficient in HE_m, h_{mcon} (W/m^2K) is calculated according to [24] as:

$$h_{mcon} = \frac{Nu_{mcon} \cdot \lambda_w}{d_{e2m}} . \tag{3.18}$$

There are:
d_{e2m} - equivalent diameter of HE_m condensation side (m);
Nu_{mcon} - condensation Nusselt number in HE_m (-).
λ_m - thermal conductivity of HE_m plate (W/mK);

The equivalent diameter of HE_m condensation side, d_{e2m} is calculated as:

$$d_{e2m} = \frac{2 \cdot b_{2m}}{\mu_m} . \tag{3.19}$$

There are:
b_{2m} - mean flow channel gap of HE_m condensation side (m);
μ_m - plate enlargement factor of HE_m (-).

The condensation Nusselt number in HE_m, Nu_{mcon} is calculated as:

$$Nu_{bw} = C \cdot \mathrm{Re}_{q2m}^{m} \cdot \mathrm{Pr}_w^{0.33} . \tag{3.20}$$

There are:
C, m - constants (-) that depend on β_m (^{o}), plate chevron angle of HE_m as C=3.77; m=0.43; when β_m=60^o and C=0.325; m=0.62; when β_m=30^o (two fixed plate chevron angle option);
Re_{q2m} - hydraulic Reynolds number of HE_m condensation side (-).

The hydraulic Reynolds number of HE_m condensation side, Re_{q2m} is calculated as:

$$\mathrm{Re}_{q2m} = \frac{G_{eq2m} \cdot d_{e2m}}{\eta_w} \ . \qquad (3.21)$$

There is:
G_{eq2m} - modified equivalent mass flux of HE_m condensation side (kg/m^{2}s).

The modified equivalent mass flux of HE_m condensation side, G_{eq2m} is calculated as:

$$G_{eq2m} = G_{2m} \cdot \left[1 - x_{2m} + x_{2m} \cdot (\frac{\rho_w}{\rho_v})^k \right] \ . \qquad (3.22)$$

There are:
k - constant (-) that depends on β_m as k=0.14; when β_m=60^o and k=0.4; when β_m=30^o;
G_{2m} - mass flux of HE_m condensation side (kg/m^{2}s);
β_m – plate chevron angle in HE_m (^{o});
x_{2m} - mean vapor quality of HE_m condensation side, x_{2m}=0.5 (condensation starts at x=1 and ends at x=0) (-);
ρ_v - vapor density at corresponding (condensation) temperature (kg/m^3).

The mass flux of HE_m condensation side, G_{2m} is calculated as:

$$G_{2m} = \frac{m_{pw}}{\frac{N_{om} - 1}{2} \cdot A_{x2m}} \ . \qquad (3.23)$$

There are:
N_{om} - number of HE_m plates (-);
A_{x2m} - cross flow channel area of HE_m condensation side (m^2).

The cross flow channel area of HE_m condensation side, Ax2m is calculated as:

$$A_{x2m} = b_{2m} \cdot w_m \ . \qquad (3.24)$$

There is:
w_m - effective width of HE_m plate (m).

The evaporation heat transfer coefficient in HE_m, h_{mevp} (W/m^{2}K) is calculated according to [23] as:

$$h_{mevp} = E_{1m} \cdot h_{11m} + S_{1m} \cdot h_{pool} \ . \qquad (3.25)$$

There are:
E_{1m}, S_{1m} - enhancement and suppression factors (-);
h_{11m} - evaporation convective heat transfer coefficient (W/m^{2}K);
h_{pool} - evaporation nucleate boiling heat transfer coefficient (W/m^{2}K).

The enhancement and suppression factor, E_{1m} is calculated as:

$$E_{1m} = 1 + 24000 \cdot Bo_{1m}^{1.16} + 1.37 \cdot (\frac{1}{X_{tt1m}})^{0.86} . \qquad (3.26)$$

There are:
Bo_{1m} - Boiling number of HE_m evaporation side (-);
X_{tt1m} - Martinelli parameter of HE_m evaporation side (-).

The boiling number of HE_m evaporation side, Bo_{1m} is calculated as:

$$Bo_{1m} = \frac{q_{1m}}{G_{1m} \cdot r_{te}} . \tag{3.27}$$

There are:
q_{1m} - heat flux of HE_m evaporation side (W/m^2);
G_{1m} - mass flux of HE_m evaporation side (kg/m^2s). The mass flux, G_{1m} is calculated according to equation (3.23), using variables: N_{om}, m_{swi} and A_{x1m}, there the cross flow channel area of HE_m evaporation side, A_{x1m} (m^2) is calculated according to equation (3.24), using variables: b_{1m} and w_m, there b_{1m} (m) is mean flow channel gap of HE_m evaporation side.
The Martinelli parameter of HE_m evaporation side, X_{tt1m} is calculated as:

$$X_{tt1m} = \left(\frac{1-x_{1m}}{x_{1m}}\right)^{0.9} \cdot \left(\frac{\rho_v}{\rho_{bw}}\right)^{0.5} \cdot \left(\frac{\eta_{bw}}{\eta_v}\right)^{0.1} . \tag{3.28}$$

There are:
x_{1m} - mean vapor quality of HE_m condensation side (evaporation starts at x=0 and ends at $x=m_{pw}/m_{swi}$) (-);
η_v - vapor dynamic viscosity at corresponding (evaporation) temperature (Pa·s).

The enhancement and suppression factor, S_{1m} is calculated as:

$$S_{1m} = \left(1 + 1.15e - 6 \cdot E_{1m}^2 \cdot \mathrm{Re}_{l1m}^{1.17}\right)^{-1} . \tag{3.29}$$

There is:
Re_{l1m} - liquid Reynolds number of HE_m evaporation side (-);

The liquid Reynolds number of HE_m evaporation side, Re_{l1m} is calculated as:

$$\mathrm{Re}_{l1m} = \frac{(1-x_{1m}) \cdot G_{1m} \cdot d_{e1m}}{\eta_{bw}} . \tag{3.30}$$

There is:
d_{e1m} - equivalent diameter of HE_m evaporation side (m).

The equivalent diameter of HE_m condensation side, d_{e1m} is calculated according to equation (3.19), using variables: b_{1m} and μ_m, there b_{1m} (m) is mean flow channel gap of HE_m evaporation side.

The evaporation convective heat transfer coefficient, h_{11m} is calculated as:

$$h_{11m} = 0.023 \cdot \mathrm{Re}_{l1m}^{0.8} \cdot \mathrm{Pr}_{bw}^{0.4} \cdot \left(\lambda_{bw}/d_{e1m}\right) . \tag{3.31}$$

The evaporation nucleate boiling heat transfer coefficient, h_{pool} is calculated as:

$$h_{pool} = 55 \cdot p_{r1m}^{0.12} \cdot \left(-\log_{10} p_{r1m}\right)^{-0.55} \cdot M^{-0.5} \cdot q_{1m}^{0.67} . \tag{3.32}$$

There are:
p_{r1m} - relative evaporation pressure, $p_{r1m}=p_e/p_c$ (-), there pc is critical water pressure, p_c=22.089 MPa;
M - molecular weight of water (kg/kmol), M=18. kg/kmol.
The presented evaporation equations are valid for $2000<Re_{l1m}<12000$ and $0.0002<Bo_{1m}<0.002$.

The one-phase convective heat transfer coefficients of brine and superheated vapor are calculated according to equations (2.22-2.30).

In those equations for h_{1mw} calculation should use followed values: b_{1m}, w_m, β_m, μ_m, N_{om}. The physical properties of brine, λ_{bw}, P_{rbw}, η_{bw} are calculated at main brine temperature as $(t_{be}+t_{swi})/2$; physical properties of brine, η_{bwall} is calculated at main wall temperature as $(t_{be}+t_{swi}+t_{crsv}+t_c)/4$. Then using (2.23), d_{e1m} is calculated, using (2.30), A_{x1m} is calculated, using (2.28), Re_{1mw}, the Reynolds number of HE_m brine is calculated, using (2.24), Nu_{1mw}, the Nusselt number of HE_m brine is calculated and finally using (2.22), h_{1mw}, convective heat transfer coefficient of brine in HE_m is calculated.

Also in those equations for h_{2mv} calculation should use followed values: b_{2m}, w_m, β_m, μ_m, N_{om}. The physical properties of superheated vapor, λ_{sv}, P_{rsv}, η_{sv} are calculated at main superheated vapor temperature as $(t_{crsv}+t_c)/2$; physical properties of superheated vapor, η_{vwall} is calculated at main wall temperature as $(t_{be}+t_{swi}+t_{crsv}+t_c)/4$. Then using (2.23), d_{e2m} is calculated, using (2.30), A_{x2m} is calculated, using (2.28), Re_{2mv}, the Reynolds number of HE_m superheated vapor is calculated, using (2.24), Nu_{2mv}, the Nusselt number of HE_m superheated vapor is calculated and finally using (2.22), h_{2mv}, convective heat transfer coefficient of superheated vapor in HE_m is calculated.

Because h_{mevp} depends on heat flux, q_{1m} and heat flux depends on evaporation heat transfer coefficient, h_{mevp}, iteration procedure is needed. When equation (3.8) is satisfied by the predicted heat flux value, the iteration procedure is finished. Then the needed flow path length of HE_m, h_m (m) can be calculated as:

$$A_{mtot} = A_{hem} + A_{hem1} + A_{hem2} = \frac{Q_{hem}}{U_{hem} \cdot \Delta t_{mm}} + \frac{Q_{hem1}}{U_{hem1} \cdot \Delta t_{mm1}} + \frac{Q_{hem2}}{U_{hem2} \cdot \Delta t_{mm2}} , \qquad (3.33)$$

$$h_m = \frac{A_{mtot}}{(N_{om} - 2) \cdot w_m} . \qquad (3.34)$$

There A_{mtot} is total HE_m heat transfer area (m^2).

4 Results and discussion

4.1 The start values of MVC mathematical model

Described MVC plant mathematical model was used to build MVC1 software. After this step, the chosen MVC plant model and simulation conditions were assumed. In further text, the used MVC characteristics and simulation conditions are described:

Constant simulation values

Sea water characteristics: salt percent, s_{p100}=3%; environmental temperature, t_{sw}=20°C.

General MVC plant characteristics: product/seawater ratio, α=0.3; recirculation brine flow ratio, α_b=0; condensation temperature, t_c=80°C.

Compressor characteristics: isentropic efficiency, η_{ic}=0.8.

One-phase heat exchangers (HE1 and HE2) characteristics: parallel connection HE1 and HE2; seawater mass flow rate, m_{sw1} is approximately equal to brine mass flow rate, m_{bw}; seawater mass flow rate, m_{sw2} is approximately equal to product water mass flow rate, m_{pw} (optimal effect of parallel HE connection); mean flow channel gap of HE1= mean flow channel gap of HE2, b_1= b_2=2.5 mm; thickness of HE1 plate = thickness of HE2 plate, δ_1= δ_2=0.6 mm; enlargement factor of HE1 plate = enlargement factor of HE2 plate, μ_1= μ_2=1.17; chevron angle of HE1 plate = chevron angel of HE2 plate, β_1= β_2 =60°; thermal conductivity of HE1 plate = thermal conductivity of HE2 plate, λ_1= λ_2 =20 W/mK (the material of plates is stainless steel).

Two-phase heat exchangers (HE_m) characteristics: counter flow in HE_m; mean flow channel gap of HE_m evaporation side = mean flow channel gap of HE_m condensation side, b_{1m}= b_{2m}=6 mm; thickness of HE_m plate, δ_m=0.6 mm; enlargement factor of HE_m plate, μ_m=1.17; chevron angle of HE_m plate, β_m=60°; thermal conductivity of HE_m plate, λ_m= 20 W/mK (the material of plates is stainless steel ion-implanted or not); the improvement factor of evaporation, if_e=1 (filmwise condensation).

Variable simulation values

Same characteristic and conditions of MVC model have taken two to five different values.

General MVC plant characteristics: evaporation temperature, t_e=76°C, 73°C, 70°C, 67°C and 64°C (condensation-evaporation temperature difference, t_c-t_e=4°C, 7°C, 10°C, 13°C and 16°C); MVC plant capacity, Q_{MVC}=100 m^3/day, 200 m^3/day, 300 m^3/day.

One-phase heat exchangers (HE1 and HE2) characteristics: values of effective width of plate and number of plates depend on chosen plant capacity (Q_{MVC}) according to scheme: for Q_{MVC}=100 m^3/day: effective width of HE1 plate, w_1=0.35 m; effective width of HE2 plate, w_2=0.3 m; number of HE1 plates, N_{o1}=71; number of HE2 plates, N_{o1}=51; for Q_{MVC}=200 m^3/day: w_1=0.5 m; w_2=0.4 m; N_{o1}=91; N_{o1}=51; for Q_{MVC}=300 m^3/day: w_1=0.6 m; w_2=0.4 m; N_{o1}=101; N_{o1}=71; All defined values were adjusted to a minimum of Reynolds number for providing of turbulent flow in HE1 and HE2 (Re_{bw}, Re_{sw1}, Re_{pw}, Re_{sw2}). Assumed limit value of Re numbers was 500 (exceptionally 450).

Two-phase heat exchangers (HE_m) characteristics: values of effective width of plate and number of plates depend on chosen plant capacity (Q_{MVC}) according to scheme: for Q_{MVC}=100 m^3/day: effective width of HE_m plate, w_m=0.4 m; number of HE_m plates, N_{om}=71; for Q_{MVC}=200 m^3/day: w_m=0.5 m; N_{om}=91; for Q_{MVC}=300 m^3/day: w_m=0.6 m; N_{om}=101; All defined values were adjusted to a evaporation liquid Reynolds number and evaporation boiling number range for validation of calculation data (see [23]) in evaporation side of HE_m (2000<Re_{l1m}<12000 and 0.0002<Bo_{1m}<0.002). Two values of improvement factor of condensation, if_c are assumed: if_c=1 for stainless steel plates (filmwise condensation) and if_c=5 for ion-implanted stainless steel plates (dropwise condensation).

4.2 Simulation results

Using values described in previous chapter, the planed simulation data were obtained.

One phase heat exchangers are very important part of MVC plant. Compressor power should be spent only on providing a temperature difference needed for condensation-evaporation heat transfer. If the HE_m inlet temperature of sea water is lower than calculated value (see equation (3.7)), compressor has to compensate this shortage by additional power. This is not mission of compressor than one-phase heat exchangers. Because the available temperature differences between brine, product water and sea water (heat transfer driving force) are small the one-phase heat exchangers must have a large heat transfer areas. Figure 1 shows the influence of temperature difference of condensation-evaporation (c-e) side to total heat transfer area of MVC one-phase heat exchangers. Simulation cases are carried out for three MVC plant capacities (100, 200 and 300 m^3/day). Effect of condensation heat transfer improvement (if_c=5) does not influence on one-phase heat exchangers functioning. The one-phase heat transfer areas significantly decrease by temperature difference of condensation-evaporation (c-e) side increasing but this trend also demands a compressor power increasing (an electrical energy consumption increasing). Bigger MVC plant capacity means bigger one-phase heat transfer areas.

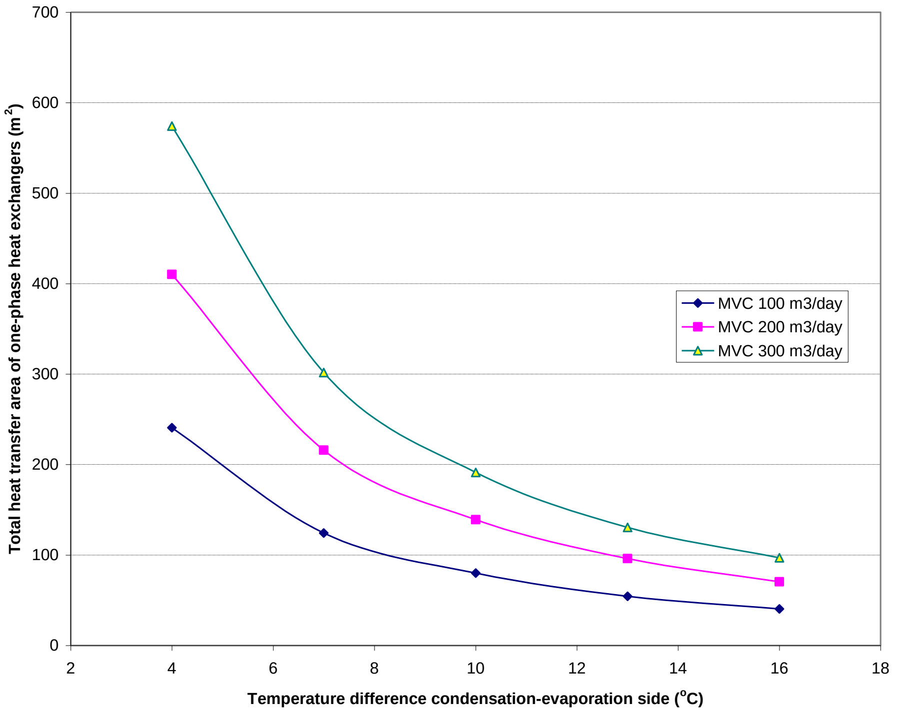

Fig. 1 The influence of temperature difference of condensation-evaporation side to total heat transfer area of MVC one-phase heat exchangers

Figure 2 shows the influence of temperature difference of condensation-evaporation side to the compressor power demanded, P_{rc} and specific electrical energy consumption of MVC plant, E_{sc}. The usual and recommended E_{sc} values are in range between 7 kWh/m^3 and 12 kWh/m^3 ([26]). This means that MVC plant operative range of c-e temperature difference, Δt_{mm} is placed between 4^{o}C and 6^{o}C, approximately. Certainly, under specific conditions the bigger specific electrical energy consumption can be acceptable ([27]). Usually, the electrical energy consumption are the biggest part of a MVC plant product water price. Good functioning of MVC plant under small c-e temperature difference demands an improvement of c-e heat transfer process.

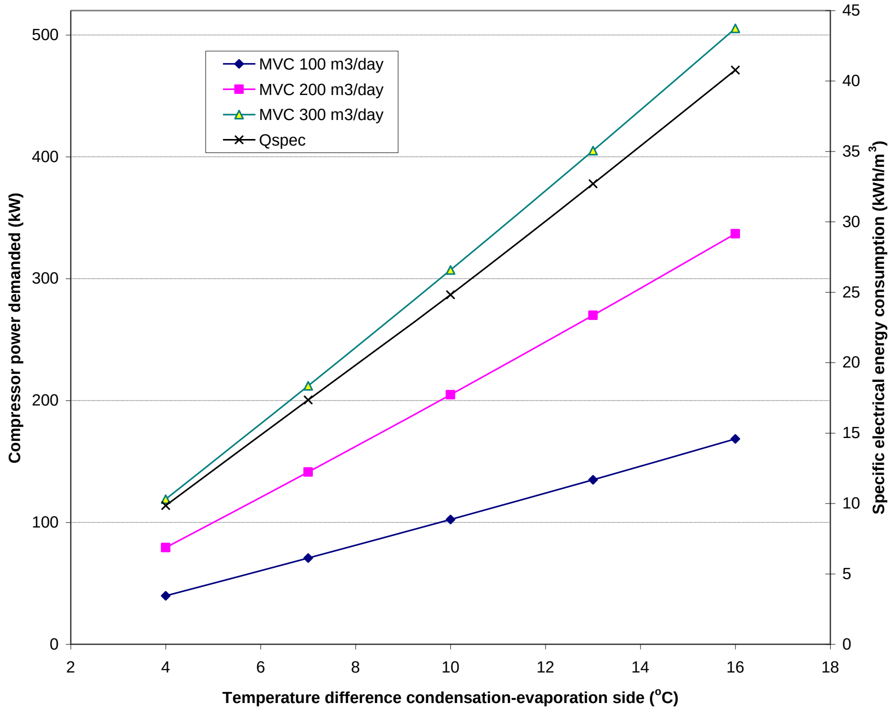

Fig. 2 The influence of temperature difference of condensation-evaporation side to the compressor power demanded and specific electrical energy consumption of MVC plant

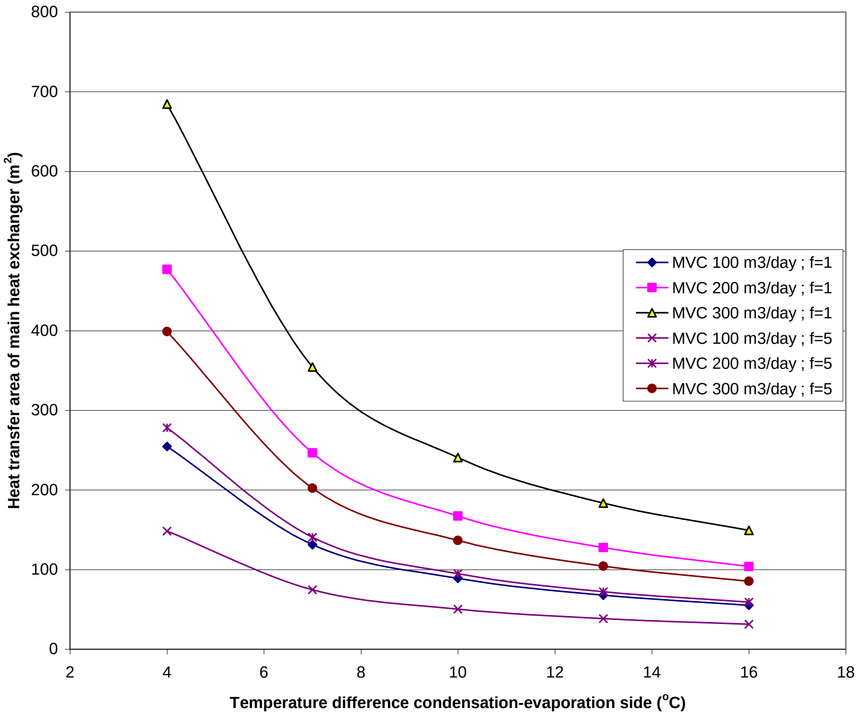

Fig. 3 The influence of temperature difference of condensation-evaporation side to the heat transfer area of MVC main heat exchanger for filmwise (if_c=1) and dropwise (if_c=5) condensation

Figure 3 shows the effects of condensation heat transfer improvement by ion-implanted metallic (iim) surface on size of HE_m heat transfer area. Using iim surface and improvement factor of dropwise condensation, if_c=5 the significant reduction of HE_m heat transfer area is obtained for all three presented MVC plant capacity. For if_c=5 and Q_{MVC}=300 m^3/day simulation case the total HE_m heat transfer area, A_{mtot} is smaller even than A_{mtot} for if_c=1 and Q_{MVC}=200 m^3/day simulation case. For smaller capacity (Q_{MVC}=100 m^3/day) the decreasing effect of A_{mtot} using iim surface (dropwise condensation) are smaller in absolute values of A_{mtot}. Both curves for Q_{MVC}=100 m^3/day are placed under curve for Q_{MVC}=200 m^3/day and dropwise condensation (if_c=5).

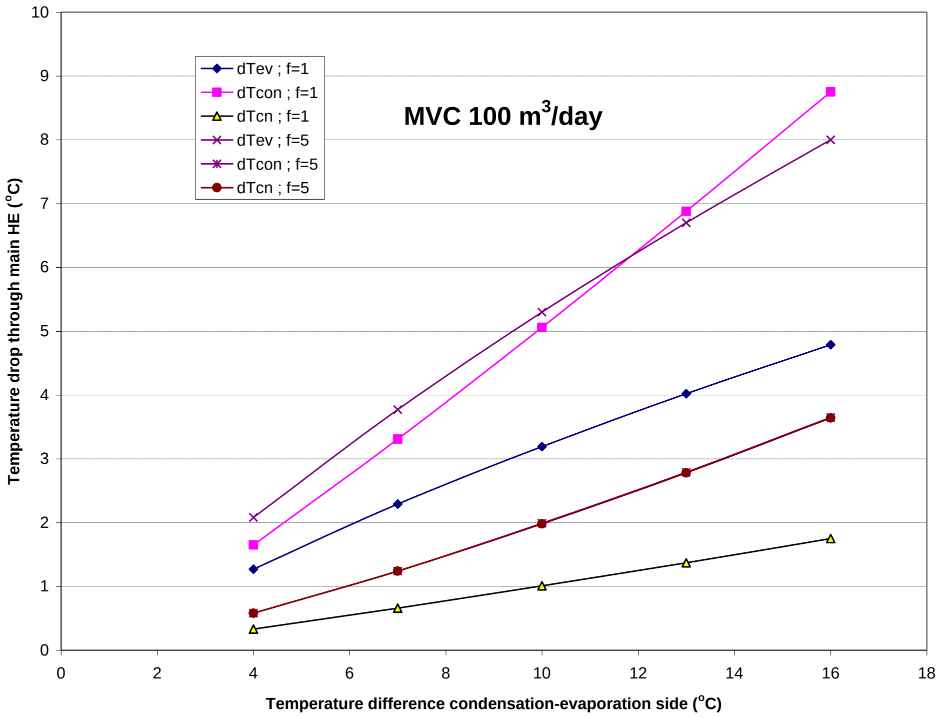

Fig. 4 The influence of temperature difference of condensation-evaporation side to the temperature drops through MVC main heat exchanger (evaporation, wall conduction and condensation) for filmwise (if_c=1) and dropwise (if_c=5) condensation and MVC plant capacity, Q_{MVC}=100 m^3/day

Figures 4 and 5 show the influence of temperature difference of condensation-evaporation side to the temperature drops through MVC main heat exchanger (evaporation, wall-conduction and condensation) for filmwise (if_c=1) and dropwise (if_c=5) condensation and MVC plant capacity, Q_{MVC}=100 m^3/day; 300 m^3/day, respectively. Total temperature difference between condensation and evaporation side in main heat exchanger (HE_m) is divided on particular temperature drops: evaporation, dT_{ev}, wall-conduction, dT_{cn} and condensation dT_{con}. The sum of those drops always has to be equal the total c-e temperature difference, Δt_{mm}. A bigger temperature drop means a bigger thermal resistance. In case of filmwise condensation (if_c=1), condensation process makes the biggest thermal resistance in HE_m and on other side, wall-conduction thermal resistance (stainless still) is insignificant. In case of dropwise condensation (if_c=5), the most significant temperature drop is placed on evaporation side, while other two drops (dt_{cn} and dt_{con}) are merged for Q_{MVC}=100 m^3/day or very close for Q_{MVC}= 300 m^3/day. Evaporation temperature drop curves has different trend than other because the evaporation heat transfer coefficient directly depends on heat flux value (see equation (3.25)-(3.32)). In fact, improvement of condensation process in HE_m has double effect. The dropwise condensation strongly influences on evaporation process, arising the evaporation heat flux and evaporation heat transfer coefficient. Especially for bigger MVC plant capacities, wall-conduction temperature drop becomes more significant than condensation temperature drop and activities as decreasing of HE_m plate thickness or using more conductive plate material could be very effective.

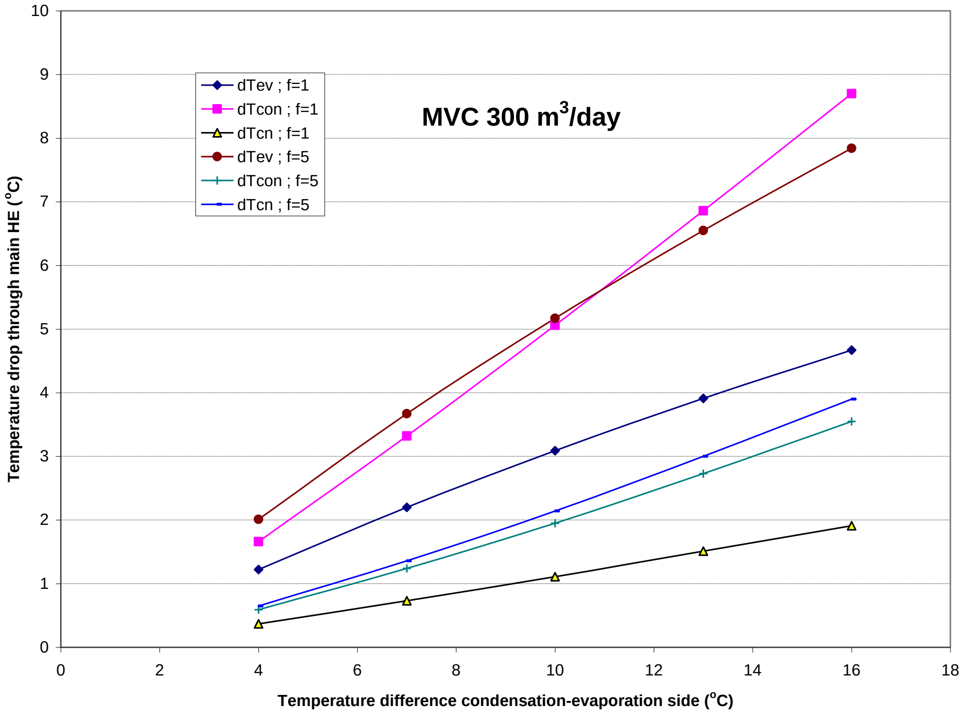

Fig. 5 The influence of temperature difference of condensation-evaporation side to the temperature drops through MVC main heat exchanger (evaporation, wall conduction and condensation) for filmwise (if_c=1) and dropwise (if_c=5) condensation and MVC plant capacity, Q_{MVC}=300 m^3/day

5. Conclusion

In MVC desalination plant a dropwise condensation can have a double improvement effect on heat transfer process. For assumed improvement factor of dropwise condensation, comparing with filmwise condensation by the same MVC plant capacity, the reduction of main heat exchanger area is within 40% and 45%. Of course, more investigations are needed to achieve additional information about an ion-implanted metallic surface influence to condensation and evaporation process in small channels (plate heat exchangers), under variable Re-numbers and vapor qualities.

6 References

[1] Semiat R., Desalination: Present and Future, Water International, 2000; 25(1):54-65.
[2] Veza J.M., Mechanical vapour compression desalination plants - A case study, Desalination, 1995; 101:1-10.
[3] Aybar H.S., Analysis of a mechanical vapor compression desalination system, Desalination, 2002; 142:181-186.

[4] Al-Juwayhel F.,El-Dessouky H.,Ettouney H., Analysis of single-effect evaporator desalination system combined with vapor compression heat pumps, Desalination, 1997; 114:253-275.
[5] Gunzbourg J., Larger D., Cogeneration applied to very high efficiency thermal seawater desalination plants, Desalination, 1999; 125:203-208.
[6] Virk G.S.,Ford M.G.,Denness B.,Ridett A., Hunter A., Ambient energy for low-cost water desalination, Desalination, 2001; 137:149-156.
[7] Slasarenko V.V., Heat pumps as a source of heat energy for desalination of seawater, Desalination, 2001; 139:405-410.
[8] Witte T.,Siegfriedsen S., El-Allawy M., Direct use of wind energy for seawater desalination by vapour compression or reverse osmosis, Desalination, 2003; 156:275-279.
[9] Karameldin A., Lotfy A., Mekhemar S., The Red Sea area wind-driven mechanical vapor compression desalinataion system, Desalination, 2002; 153:47-53.
[10] Legorreta C., Hinge S., Tonner J., Lovato A., Plates-the next breakthrough in desalination, Desalination, 1999; 122:235-246.
[11] Muller-Steinhagen H., Zhao Q., Investigation of low fouling surface alloys made by ion implantation technology, Chemical Engineering Science, 1997; 52(19):3321-3332.
[12] Koch G., Kraft K., Leipertz A., Parameter stydy on the performance of dropwise condensation, Rev. Gen. Therm., 1998; 37:539-548.
[13] Koch G., Zhang D.C., Leipertz A., Grischke M., Trojan K., Dimigen H., Study on plasma enhanced CVD coated material to promote dropwise condensation of steam, Int. J. Heat Mass Transfer, 1998; 41(13):1899-1906.
[14] Muley A., Manglik R.M., Experimental Study of Turbulent Flow Heat Transfer and Pressure Drop in a Plate Heat Exchanger With Chevron Plates, ASME, Journal of Heat Transfer, 1999; 121:110-117.
[15] Hsieh Y.Y., Chiang L.J., Lin T.F., Subcooled flow boiling heat transfer of R-134a and the associated bubble characteristics in a vertical plate heat exchanger, Int. J. Heat Mass Transfer, 2002; 45:1791-1806.
[16] Jung D., Kim Y., Ko Y., Song K., Nucleate boiling heat transfer coefficients of pure halogenated refrigerants, Int. J. Refrigeration, 2003; 26:240-248.
[17] Yan Y.Y., Lin T.F., Evaporation heat transfer and pressure drop of refrigerant R-134a in a small pipe, Int. J. Heat Mass Transfer, 1998; 41:4183-4194.
[18] Han D.H., Lee K.J., Kim Y.H., Experiments on the characteristics of evaporation of R410A in brazed plate heat exchangers with different geometric configurations, Applied Thermal Engineering, 2003; 23:1209-1225.
[19] Hsieh Y.Y., Lin T.F., Satau rated flow boiling heat transfer and pressure drop of refrigerant R410A in a vertical plate heat exchanger, Int. J. Heat Mass Transfer, 2002; 45:1033-1044.
[20] Yan Y.Y., Lio H.C., Lin T.F., Condensation heat transfer and pressure drop of refrigerant R-134a in a plate heat exchanger, Int. J. Heat Mass Transfer, 1998; 42:993-1006.
[21] Yan Y.Y., Lin T.F., Condensation heat transfer and pressure drop of refrigerant R-134a in a small pipe, Int. J. Heat Mass Transfer, 1999; 42:697-708.
[22] Wen D.S., Yan Y., Kenning D.B.R., Saturated flow boiling of water in a narrow channel: time-averaged heat transfer coefficients and correlations, Applied Thermal Engineering, 2004; 24:1207-1223.

[23] Hsieh Y.Y., Lin T.F., Evaporation Heat Transfer nad Pressure Drop of Refrigerant R410A Flow in a Vertical Plate Heat Exchanger, ASME, Journal of Heat Transfer, 2003; 125:852-857.
[24] Wurfel R., Ostrowski N., Experimental investigations of heat transfer and pressure drop during the condensation process within plate heat exchangers of the herringbone-type, Int. J. Thermal Sciences, 2004; 43:59-68.
[25] Lukic N., Leipertz A., Diezel L., Froba A.P., Mechanical vapor commpresion desalination software MVC1, ESYTEC Energie und Systemtechnik GmbH Erlangen, 2004.
[26] Buros O.K., The ABCs of Desalting, Second Edition, International Desalination Association, Topsfield, Massachusetts, USA.
[27] Zyclodest, Product information, EnviTech GmbH, Mindelheim, Germany.